

# Spectral areas and ratios classifier algorithm for pancreatic tissue classification using optical spectroscopy

Malavika Chandra,<sup>a</sup> James Scheiman,<sup>b,c</sup>  
Diane Simeone,<sup>c,d</sup> Barbara McKenna,<sup>e</sup> Julianne Purdy,<sup>e</sup>  
and Mary-Ann Mycek<sup>a,c,f</sup>

<sup>a</sup>University of Michigan, Applied Physics Program, Ann Arbor, Michigan 48109-1040

<sup>b</sup>University of Michigan, Department of Internal Medicine, Ann Arbor, Michigan 48109-0362

<sup>c</sup>University of Michigan, Comprehensive Cancer Center, Ann Arbor, Michigan 48109-0944

<sup>d</sup>University of Michigan, Department of Surgery, Ann Arbor, Michigan 48109-5331

<sup>e</sup>University of Michigan, Department of Pathology, Ann Arbor, Michigan 48109-0602

<sup>f</sup>University of Michigan, Department of Biomedical Engineering, Ann Arbor, Michigan 48109-2099

**Abstract.** Pancreatic adenocarcinoma is one of the leading causes of cancer death, in part because of the inability of current diagnostic methods to reliably detect early-stage disease. We present the first assessment of the diagnostic accuracy of algorithms developed for pancreatic tissue classification using data from fiber optic probe-based bimodal optical spectroscopy, a real-time approach that would be compatible with minimally invasive diagnostic procedures for early cancer detection in the pancreas. A total of 96 fluorescence and 96 reflectance spectra are considered from 50 freshly excised tissue sites—including human pancreatic adenocarcinoma, chronic pancreatitis (inflammation), and normal tissues—on nine patients. Classification algorithms using linear discriminant analysis are developed to distinguish among tissues, and leave-one-out cross-validation is employed to assess the classifiers' performance. The spectral areas and ratios classifier (SpARC) algorithm employs a combination of reflectance and fluorescence data and has the best performance, with sensitivity, specificity, negative predictive value, and positive predictive value for correctly identifying adenocarcinoma being 85, 89, 92, and 80%, respectively. © 2010 Society of Photo-Optical Instrumentation Engineers. [DOI: 10.1117/1.3314900]

Keywords: spectroscopy; fluorescence; reflectance; tissues; pancreas; carcinoma.

Paper 09379LRR received Aug. 26, 2009; revised manuscript received Jan. 7, 2010; accepted for publication Jan. 18, 2010; published online Feb. 18, 2010.

Pancreatic adenocarcinoma has a five-year survival rate of only 5%, making it the fourth leading cause of cancer death in the United States.<sup>1</sup> Current diagnostic procedures are unable to reliably diagnose early stage disease.<sup>2</sup> Endoscopic

ultrasound-guided fine needle aspiration (EUS-FNA), an established method for the diagnosis of pancreatic adenocarcinoma, has only 54% sensitivity for detecting cancer in the setting of pancreatitis (inflammation)<sup>3</sup> and an “unacceptably low” reliability at ruling out malignancy.<sup>2</sup> Reliably detecting the disease in its early stages and distinguishing it from pancreatitis could greatly improve the chances of patient survival.

Fluorescence and reflectance spectroscopies have been applied in combination to detect oral cancer,<sup>4</sup> breast cancer,<sup>5</sup> dysplasia in Barrett's esophagus,<sup>6</sup> and cervical cancer.<sup>7</sup> The two spectroscopies can provide complimentary information about biological tissue, with reflectance spectroscopy providing information primarily about tissue morphology (including the size and density of cell nuclei), while fluorescence reports mainly on tissue biochemistry (including intra- and extracellular endogenous fluorophores like NAD(P)H and collagen).

Previously, we reported the first fluorescence and reflectance measurements of *ex vivo* human pancreatic tissues and *in vivo* human pancreatic cancer xenografts in mice.<sup>8</sup> Here, we report for the first time the diagnostic accuracy of pancreatic tissue classification algorithms employing fluorescence data alone, reflectance data alone, or a combination of the two, to determine whether both reflectance and fluorescence information was necessary for optimal tissue classification. Optical spectra were measured from freshly excised pancreatic tissues obtained during pancreatic surgeries. Prototype, clinically compatible optical technology<sup>8,9</sup> was employed to study 50 tissue sites from nine patients (average age  $62 \pm 11$  years; 7 female, 2 male) within 30 min of tissue excision. Briefly, a 355-nm pulsed laser and a cw lamp were light sources for fluorescence and reflectance spectroscopies, respectively. A fiber probe was employed for light delivery to and collection from tissue. Collected photons were directed to a spectrograph-coupled intensified charge-coupled device camera for spectral detection. After optical data acquisition from each measurement site, tissue at the site was removed for histopathological analysis. The study was approved by the Institutional Review Board of the University of Michigan Medical School, and patient consent was obtained.

Acquired fluorescence spectra in the 360 to 750 nm range were corrected for spectral instrument response after background correction.<sup>10</sup> Reflectance spectra were background subtracted ( $R$ ) and then scaled by the lamp reflectance spectrum ( $R_o$ ) to obtain corrected reflectance spectra ( $R/R_o$ ) in the 400 to 750 nm spectral range.<sup>9</sup> All spectra were then normalized by scaling the peak intensity value to unity. Two sets of fluorescence and reflectance measurements were made on each site, except one. Three pairs of fluorescence and reflectance spectra were excluded based on the exclusion criteria: ratio of reflectance  $R_{550}/R_{600} < 0.1$  or fluorescence signal-to-noise ratio (SNR)  $< 25$ , where  $SNR = (\text{average intensity between } 470 \text{ and } 500 \text{ nm}) / (\text{standard deviation of intensity between } 700 \text{ and } 750 \text{ nm})$ . This left 96 fluorescence and 96 reflectance measurements: 33 fluorescence and reflectance measurements were made on 17 adenocarcinoma sites, 41 were made on 22 pancreatitis sites, and 22 were made on 11 normal sites.

Figure 1 shows the mean of normalized measured reflectance and fluorescence spectra for adenocarcinoma (red

Address all correspondence to: Mary-Ann Mycek, University of Michigan, 1101 Beal Avenue, Ann Arbor Michigan 48109-2099. Tel: 734-647-1361; E-mail: mycek@umich.edu.

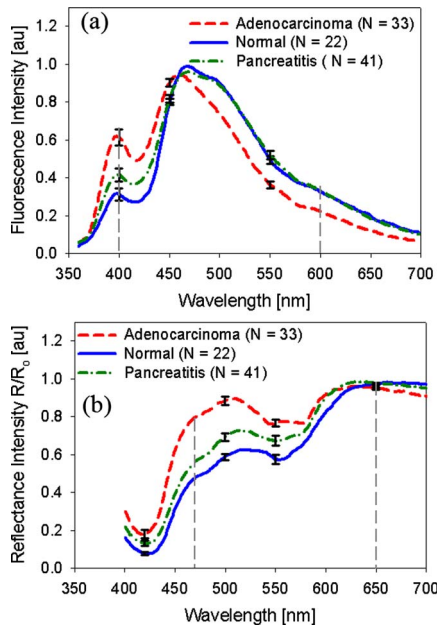


**Fig. 1** (a) Mean fluorescence spectra obtained from human pancreatic normal (blue solid line), pancreatitis (green dot-dash line), and adenocarcinoma (red dashed line) tissues. The gray vertical dashed lines indicate the wavelengths at which  $F_{ratio}(=F_{400}/F_{600})$  was calculated for each spectrum. (b) Mean reflectance spectra obtained from normal (blue solid line), pancreatitis (green dot-dash line), and adenocarcinoma (red dashed line) tissues. The gray dashed lines indicate the wavelengths at which  $R_{ratio}(=R_{470}/R_{650})$  was calculated for each spectrum.  $N$  denotes the number of individual spectra. The standard error is shown at select wavelengths. (Color online only.)

dashed line), pancreatitis (green dot-dashed line), and normal (blue solid line) pancreatic tissues, along with the standard error at select wavelengths. Tissue fluorescence spectra revealed cellular NAD(P)H (emission around 460 nm) and extracellular matrix collagen (emission around 400 nm), and characteristic hemoglobin absorption dips at around 420, 540, and 575 nm in the reflectance and fluorescence spectra.<sup>4-8</sup> The adenocarcinoma sites showed markedly higher reflectance than pancreatitis and normal tissue sites between 450 to 540 nm, higher fluorescence at around 400 nm, and lower fluorescence between 450 to 700 nm. Due to the *ex vivo* nature of the study, it is difficult to draw conclusions on differing hemoglobin absorption between tissue types. The observed spectral differences are consistent with increased cellular nuclear size and collagen content in pancreatic adenocarcinoma tissues.<sup>11</sup> To classify the tissue spectra based on these apparent differences, the ratio  $R_{ratio}=R_{470}/R_{650}$  was calculated for each reflectance spectrum, the wavelength integrated fluorescence ( $F_{area}$ ) was calculated as the area under each normalized fluorescence spectrum, and the ratio  $F_{ratio}=F_{400}/F_{600}$ , was calculated for each fluorescence spectrum. The gray dashed lines in Fig. 1 indicate the wavelength at which the ratios  $R_{ratio}$  and  $F_{ratio}$  were calculated.

Three different sets of these calculated spectral parameters (classification variables) were employed to develop tissue classification algorithms for distinguishing: 1. adenocarcinoma (A) from pancreatitis (P) and normal (N) tissue, 2. A from P tissue, 3. A from N tissue, and 4. P from N tissue. A leave-one-out cross-validation was undertaken to test the per-

**Table 1** RSpARC algorithm—reflectance only.

Tissue type	Sensitivity (%)	Specificity (%)	NPV (%)	PPV (%)
A versus P and N	85	86	92	76
A versus P	85	83	87	80
A versus N	88	95	84	97
P versus N	56	82	50	85

formance of the proposed tissue classification algorithms. Linear discriminant analysis (LDA) was employed using SPSS software (SPSS, Chicago, Illinois) to classify the test data using the three different sets of classification variables. LDA employs a linear combination of the classification variables to classify data. This process was repeated for each spectrum, and the sensitivity, specificity, negative predictive value (NPV), and positive predictive value (PPV) of the classification algorithms were calculated.

The first classification algorithm, the reflectance spectral areas and ratios (RSpARC) classifier employed  $R_{ratio}$  as the sole classification variable for LDA, and Table 1 gives the algorithm's performance. The second algorithm, the fluorescence spectral areas and ratios (FSpARC) classifier employed  $F_{area}$  and  $F_{ratio}$  as the classification variables for LDA, and Table 2 gives that algorithm's performance. In the third algorithm, the spectral areas and ratios (SpARC) classifier step-wise LDA was performed using minimization of Wilks' lambda ( $\Lambda$ ) criterion (P-to-enter 0.085; P-to-remove 0.1) to assess the discriminating power of the variables, and to select the best set of variables from  $R_{ratio}$ ,  $F_{area}$ , and  $F_{ratio}$  for classification. The variables retained by the step-wise analysis were then employed to classify the data. Table 3 shows the performance of this algorithm, along with the variables retained for each classification. For example, classification of A versus P employed  $R_{ratio}$ . For A versus (P and N) and P versus N classification, the combination of classifiers extracted from both reflectance and fluorescence (Table 3) performed better than using information from either just reflectance (Table 1) or just fluorescence (Table 2), indicating that for the SpARC algorithm, both fluorescence and reflectance spectroscopies are required for accurate pancreatic tissue classification.

**Table 2** FSpARC algorithm—fluorescence only.

Tissue type	Sensitivity (%)	Specificity (%)	NPV (%)	PPV (%)
A versus P and N	55	89	79	72
A versus P	52	88	69	77
A versus N	58	91	59	90
P versus N	56	64	44	74

**Table 3** SpARC algorithm—reflectance and fluorescence. Classification parameters: 1.  $R_{ratio}$ , 2.  $F_{ratio}$ , and 3.  $F_{area}$ .

Tissue type	Sensitivity (%)	Specificity (%)	NPV (%)	PPV (%)
A versus P and N <sup>1,2</sup>	85	89	92	80
A versus P <sup>1</sup>	85	83	87	80
A versus N <sup>1</sup>	88	95	84	97
P versus N <sup>1,3</sup>	61	73	50	81

Hartwig et al.<sup>2</sup> conducted a meta-analysis of 28 EUS-FNA studies, and reported median (range) values of sensitivity at 83% (54 to 96%); specificity 100% (71 to 100%); NPV 72% (16 to 92%); and PPV 100% (92 to 100%) for adenocarcinoma distinction from normal tissue and chronic pancreatitis. The performance of the SpARC algorithm for adenocarcinoma distinction from normal tissue and chronic pancreatitis (Table 3, row 1) is comparable to that of the reported performance of EUS-FNA. Fritscher-Ravens et al.<sup>3</sup> studied patients having both adenocarcinoma and pancreatitis, and reported that EUS-FNA had 54% sensitivity, 100% specificity, 91% NPV, and 100% PPV for distinguishing adenocarcinoma from pancreatitis in the setting of pancreatitis. All adenocarcinoma measurements in the study reported here were also made on pancreata that had concurrent histologic pancreatitis in addition to the carcinoma. Thus, the sensitivity of SpARC (85%) (Table 3 row 2) is well above that of EUS-FNA (54%)<sup>3</sup> for distinguishing adenocarcinoma from pancreatitis in the setting of pancreatitis, which is an unmet clinical need in pancreatic cancer detection. The receiver operating curves for A versus (P and N) and A versus P classification using the SpARC algorithm were calculated using SPSS software and are shown in Fig. 2. The blue line suggests that in achieving a specificity of close to 100%, the A versus P sensitivity would be comparable to EUS-FNA. Thus, employing an optical technique to guide EUS-FNA could improve the sensitivity of pancreatic adenocarcinoma detection in the setting of pancreatitis.

While this study was undertaken in an *ex vivo* setting, the

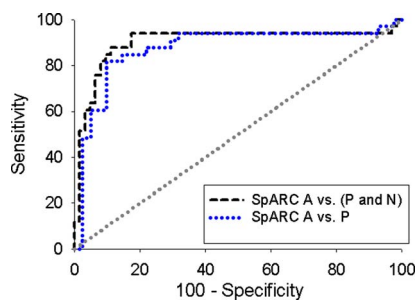


**Fig. 2** The receiver operating curves (ROCs) for A versus (P and N) (black dashed line) and A versus P classification (blue dotted line) using the SpARC algorithm, where the areas under the ROCs were  $0.901 \pm 0.043$  and  $0.874 \pm 0.047$ , respectively. The gray dotted line indicates the line of no discrimination. (Color online only.)

performance of the developed classification algorithm shows promise for clinical pancreatic tissue classification using bimodal optical spectroscopy. Although the SpARC algorithm is rapid and simple to implement, its performance may be limited because it utilizes information at only select wavelengths. Future work will include the investigation of algorithms that consider information at all wavelengths for tissue classification. Separate studies are also underway to employ parameters extracted from a photon-tissue interaction model for tissue classification.<sup>11</sup> The model provides quantitative links between spectroscopic measurements and biophysical tissue characteristics, including hemoglobin absorption. Future work will involve data acquisition *in vivo*, with the aim of deploying the fiber optic probe through a needle for optically guided EUS-FNA.

*Acknowledgments*

This work was supported in part by the National Institutes of Health (CA-114542), The National Pancreas Foundation, the Wallace H. Coulter Foundation, the University of Michigan Comprehensive Cancer Center, and the University of Michigan Medical School Translational Research Program. We thank C. Sonnenday and L. M. Colletti for allowing us to collect data during the pancreatic surgeries performed by them.

*References*

1. "Cancer Statistics 2009," see <http://www.cancer.org>.
2. W. Hartwig, L. Schneider, M. K. Diener, F. Bergmann, M. W. Buchler, and J. Werner, "Preoperative tissue diagnosis for tumours of the pancreas," *Br. J. Surg.* **96**, 5–20 (2009).
3. A. Fritscher-Ravens, L. Brand, W. T. Knofel, C. Bobrowski, T. Topalidis, F. Thonke, A. de Werth, and N. Soehendra, "Comparison of endoscopic ultrasound-guided fine needle aspiration for focal pancreatic lesions in patients with normal parenchyma and chronic pancreatitis," *Am. J. Gastroenterol.* **97**, 2768–2775 (2002).
4. M. G. Muller, T. A. Valdez, I. Georgakoudi, V. Backman, C. Fuentes, S. Kabani, N. Laver, Z. Wang, C. W. Boone, R. R. Dasari, S. M. Shapshay, and M. S. Feld, "Spectroscopic detection and evaluation of morphologic and biochemical changes in early human oral carcinoma," *Cancer* **97**, 1681–1692 (2003).
5. Z. Volynskaya, A. S. Haka, K. L. Bechtel, M. Fitzmaurice, R. Shenk, N. Wang, J. Nazemi, R. R. Dasari, and M. S. Feld, "Diagnosing breast cancer using diffuse reflectance spectroscopy and intrinsic fluorescence spectroscopy," *J. Biomed. Opt.* **13**, 024012 (2008).
6. I. Georgakoudi and M. S. Feld, "The combined use of fluorescence, reflectance, and light-scattering spectroscopy for evaluating dysplasia in Barrett's esophagus," *Gastrointest Endosc Clin. N. Am.* **14**, 519–537 (2004).
7. S. K. Chang, Y. N. Mirabal, E. N. Atkinson, D. Cox, A. Malpica, M. Follen, and R. Richards-Kortum, "Combined reflectance and fluorescence spectroscopy for *in vivo* detection of cervical pre-cancer," *J. Biomed. Opt.* **10**, 024031 (2005).
8. M. Chandra, J. Scheiman, D. Heidt, D. Simeone, B. McKenna, and M. A. Mycek, "Probing pancreatic disease using tissue optical spectroscopy," *J. Biomed. Opt.* **12**, 060501 (2007).
9. M. Chandra, K. Vishwanath, G. D. Fichter, E. Liao, S. J. Hollister, and M. A. Mycek, "Quantitative molecular sensing in biological tissues: an approach to noninvasive optical characterization," *Opt. Express* **14**, 6157–6171 (2006).
10. J. D. Pitts and M. A. Mycek, "Design and development of a rapid acquisition laser-based fluorometer with simultaneous spectral and temporal resolution," *Rev. Sci. Instrum.* **72**, 3061–3072 (2001).
11. R. H. Wilson, M. Chandra, J. Scheiman, D. Simeone, B. McKenna, J. Purdy, and M.-A. Mycek, "Optical spectroscopy detects histological hallmarks of pancreatic cancer," *Opt. Express* **17**, 17502–17516 (2009).